

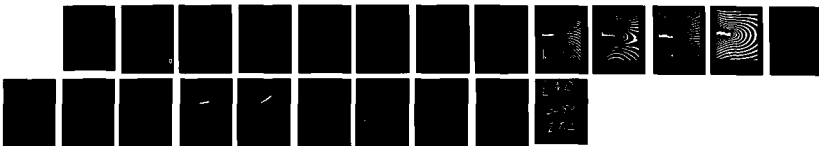
AD-A207 578

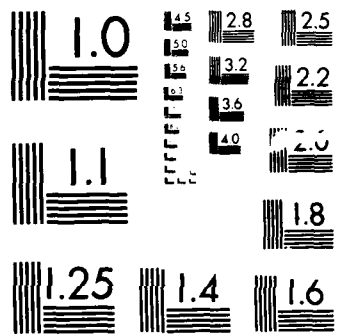
HRR FIELD IN AN ALUMINUM SEN SPECIMEN(U) WASHINGTON
UNIV SEATTLE DEPT OF MECHANICAL ENGINEERING
M S DADKHAH APR 89 UWA/DME/TR-89/63 N00014-89-J-1276

1/1

UNCLASSIFIED

F/G 11/6 1 NL





MICROCOPY RESOLUTION TEST CHART
NATIONAL BUREAU OF STANDARDS-1963-A

4

AD-A207 578

Office of Naval Research
Contract N00014-89-J-1276
Technical Report No. UWA/DME/TR-89/63
HRR FIELD IN AN ALUMINUM SEN SPECIMEN

by

M.S. Dadkhah and A.S. Kobayashi

April 1989

The research reported in this technical report was made possible through support extended to the Department of Mechanical Engineering, University of Washington, by the Office of Naval Research under Contract N00014-89-J-1276. Reproduction in whole or in part is permitted for any purpose of the United States Government.

Department of Mechanical Engineering
College of Engineering
University of Washington

DTIC
ELECTE
MAY 10 1989
S
cb E D

This document has been approved
for public release and sale in
distribution is unlimited.

89 5 10 036

HRR FIELD IN AN ALUMINUM SEN SPECIMEN

Mahyar Dadkhah* and Albert S. Kobayashi**

ABSTRACT

Moire interferometry was used to record simultaneously the vertical and horizontal displacements associated with stable crack growth in single edge notched, 2024-0 aluminum specimens. For a small stable crack growth of 1.5 mm, the vertical displacement showed the dominance of the HRR field but the horizontal displacement deviated from the HRR field at the early stage of loading. *Keywords: crack propagation; moire interferometry; HRR*

INTRODUCTION

During the past two years, the authors and their colleagues have used an improved moire interferometry technique [1] to study the path independency and the validity of the HRR [2,3] field in single edge notched, 2024-T3, 2024-0, and 5052-H32 aluminum alloy specimens subjected to uniaxial and biaxial loadings [4,5,6]. One of the objectives of this series of investigations was to study the biaxial effect on the ductile fracture criterion and thus a special cruciform specimen [4] was tested in a special biaxial testing machine [7]. The biaxiality ratio, B , was varied from the uniaxial state of $B = 0$ to the highly biaxial loading of $B = 2$. It was thought by some that the built-in bending stiffness of the cruciform specimen simulated the crack-tip state of stress found in a central notched tension specimen for which previous numerical analysis [8] showed a smaller J-dominated region. Thus the authors' previous findings that the HRR field was virtually nonexistent, except for the 2024-T3 specimens with a relatively smaller plastic yield zone, could have been attributed to the particular specimen configuration used in our studies. In particular, Shih et al. [8] has shown through numerical analysis, that a large J-dominated region existed in a single edge-notched (SEN) specimen with large scale yielding subjected to tensile and bend loadings.

The objective of this study is to determine the extent of the HRR zone in an ASTM-type single edge notched, (SEN) 2024-0 aluminum specimen.

PROCEDURES

The experimental procedure and the procedure for evaluating the J-integral have been described in detail [1,3,4] and will not be repeated for the sake of brevity. The SEN specimen used in this study is shown in Figure 1. This specimen is identical in geometry with the cruciform specimen, which was used in previous studies, with the exception that it lacks the horizontal tabs.

* Rockwell International Science Center, Thousand Oaks, CA 91360

** University of Washington, Department of Mechanical Engineering, Seattle, WA 98195

and the secondary normal strains in the directions perpendicular and parallel to the crack, respectively.

One SEN 2024-0 specimen was analyzed using the procedures described in previous publications. Figures 3 and 4 show the fringe patterns which represent the dominant v- and secondary u-displacement field, respectively, of the SEN specimen. Figure 5 and 6 show the v- and u-displacement fields, with the contours used in the J-integral calculation, of a cruciform specimen under uniaxial tension or $B = 0$. A comparison of Figures 3 and 5 and Figures 4 and 6 indicate that the v- and u-displacement fields of the SEN and uniaxially loaded cruciform specimens are identical. Figure 7 and 8 indeed show that at a reference point of $r = 1.2$ mm and $\theta = 45$, the v- and u-displacements do coincide. The u-displacement for the biaxially loaded, $B = 2$, cruciform specimen, however, differs significantly with those of the SEN and uniaxially loaded cruciform specimen.

The coincidence of the v- and u-displacement fields of the SEN and the uniaxially loaded cruciform specimens allowed the use of the J-integral values of an uniaxially loaded cruciform specimen as an estimate of the J-values of a SEN specimen. This estimation was accomplished by relating the J-value of the SEN specimen with the corresponding J-value, as shown in Figure 9, at the same vertical load of the uniaxially loaded cruciform specimen. Also shown in Figure 9 is the variation in J-values with increasing load in the biaxially loaded cruciform specimen. Despite the difference in the u-displacement field, as shown in Figure 8, the J-values for the uniaxially and biaxially loaded cruciform specimens coincide up to an applied load of 4,000 N.

Figures 11 and 12 show typical log-log plots of the variations of the v- and u-displacement, respectively with angular orientation, θ , and radial distance, r , for a load of 3290 N at which load the plastic region had penetrated the remaining ligament of the specimen. The slope of these displacement plots in the HRR region should be 0.2. The dominant v-displacement field exhibits a slope of 0.2 in a limited region circumscribing the crack tip as indicated in Figure 11. The u-displacement field, which is smaller than the v-displacement field, has an average slope of 0.51 as shown in Figure 12. The nonlinear region for the u-displacement field is considerably smaller than that of the v-displacement field.

The J-integral values shown in Figure 10 were used together with the power hardening coefficients in Figure 2 to evaluate the v- and u-displacements associated with the HRR field [2,3]. The crack tip displacements for a linearly elastic aluminum SEN specimen was also computed. Figures 13 and 14 show the measured and the computed HRR and LEFM v- and u-displacement variations, at a location of $r = 1.2$ mm and $\theta = 45$ from the crack tip, with increasing crack extension in the SEN and the cruciform specimens, respectively. The fitted curves through the measured v- and u-displacement data accentuate the closeness or difference with the HRR or LEFM displacement. The v-displacement initially followed the LEFM displacement but changed to the corresponding HRR component at higher loadings in all three specimens. The u-displacement for the SEN and uniaxially loaded cruciform specimen, on the other hand, followed the corresponding LEFM component while that of the biaxially loaded cruciform specimen followed the HRR component at the initial phase of loading.

CONCLUSION

The displacement fields near the crack tip in the cruciform and the SEN specimens used in this study were identical for all practical purposes. Thus the results generated

previously for the uniaxially loaded cruciform specimens are also applicable to the SEN specimens. As shown previously, the v-displacement followed the corresponding component of the HRR field but the u-displacement followed the corresponding component of a LEFM field for the SEN and uniaxially loaded cruciform specimens as well as during the latter phase of the biaxially loaded cruciform specimens.

DISCUSSIONS

This and previous studies [4,5,6] have consistently shown that the v-displacement outside of the nonlinear region but in the vicinity of the crack tip essentially followed the HRR field for much of the loading. The u-displacement, except for the early stage of loading in 2024-T3 specimens and biaxially loaded cruciform specimens, did not follow the HRR field and was closer or identical to the corresponding LEFM component. Thus the far-field J-integral, which was shown to be identical to the crack tip J-integral, cannot be used to characterize the crack tip states of displacement and strain. The physical significance of the J-integral from the fracture mechanics view point is therefore in need of a redefinition.

ACKNOWLEDGMENT

This research was sponsored by the Office of Naval Research under ONR Contract No. N00014-85-K-0187. The authors are indebted to Dr. Yapa Rajapakse for his support and encouragement during the course of this investigation.

REFERENCES

1. Dadkhah, M.S., Wang, F.X. and Kobayashi, A.S., "Simultaneous On-Line Measurements of Orthogonal Displacement Fields by Moire Interferometry," *Experimental Techniques*, 12, 1988, 28-30.
2. Hutchinson, J.W., "Singular Behavior at the End of a Tension Crack in a Hardening Material, *J. of the Mechanics of Physics and Solids*, 16, 1968, 13-31.
3. Rice, J.R. and Rosengren, G.F., "Plane Strain Deformation Near a Crack," *J. of the Mechanics of Physics and Solids*, 16, 1968, 1-12.
4. Dadkhah M.S., Kobayashi, A.S., Wang, F.X. and Graesser, D.L., "J-Integral Measurements Using Moire Interferometry," *Proc. of the VI Int'l Congress on Experimental Mechanics*, 1988, 227-234.
5. Dadkhah, M.S. and Kobayashi, A.S., "HRR Field of a Moving Crack: An Experimental Analysis," to be published in *Engineering Fracture Mechanics*.
6. Dadkhah, M.S. and Kobayashi, A.S., "Further Studies of a Moving Crack: An Experimental Analysis," submitted to *Journal of Plasticity*.
7. Dadkhah, M.S., "Dynamic Fracture Under the Influence of Biaxial Stress," a MS in ME thesis submitted to the University of Washington, 1984.
8. Shih, C.F., German, M.D. and Kumar, V., "An Engineering Approach for Examining Crack Growth and Stability in Flawed Structures," *Int'l J. of Pressure Vessels and Pipings*," 9, 1981, 159-196.

2. Hutchinson, J.W., "Singular Behavior at the End of a Tension Crack in a Hardening Material, J. of the Mechanics of Physics and Solids, 16, 1968, 13-31.
3. Rice, J.R. and Rosengren, G.F., "Plane Strain Deformation Near a Crack," J. of the Mechanics of Physics and Solids, 16, 1968, 1-12.
4. Dadkhah M.S., Kobayashi, A.S., Wang, F.X. and Graesser, D.L., "J-Integral Measurements Using Moire Interferometry," Proc. of the VI Int'l Congress on Experimental Mechanics, 1988, 227-234.
5. Dadkhah, M.S. and Kobayashi, A.S., "HRR Field of a Moving Crack: An Experimental Analysis," to be published in Engineering Fracture Mechanics.
6. Dadkhah, M.S. and Kobayashi, A.S., "Further Studies of a Moving Crack: An Experimental Analysis," submitted to Journal of Plasticity.
7. Dadkhah, M.S., "Dynamic Fracture Under the Influence of Biaxial Stress," a MS in ME thesis submitted to the University of Washington, 1984.
8. Shih, C.F., German, M.D. and Kumar, V., "An Engineering Approach for Examining Crack Growth and Stability in Flawed Structures," Int'l J. of Pressure Vessels and Pipings," 9, 1981, 159-196.
9. Shih, C.F., "J-Dominance Under Plane Strain Fully Plastic Conditions: The Edge Crack Plane Subjected to Combined Tension and Bending," Int'l J. of Fracture, 29, 1985, 73-84.

| | |
|--------------------|-------------------------------------|
| Accession For | |
| NTIS GRA&I | <input checked="" type="checkbox"/> |
| DTIC TAB | <input type="checkbox"/> |
| Unannounced | <input type="checkbox"/> |
| Justification | |
| By _____ | |
| Distribution/ | |
| Availability Codes | |
| Dist | Avail and/or Special |
| A-1 | |



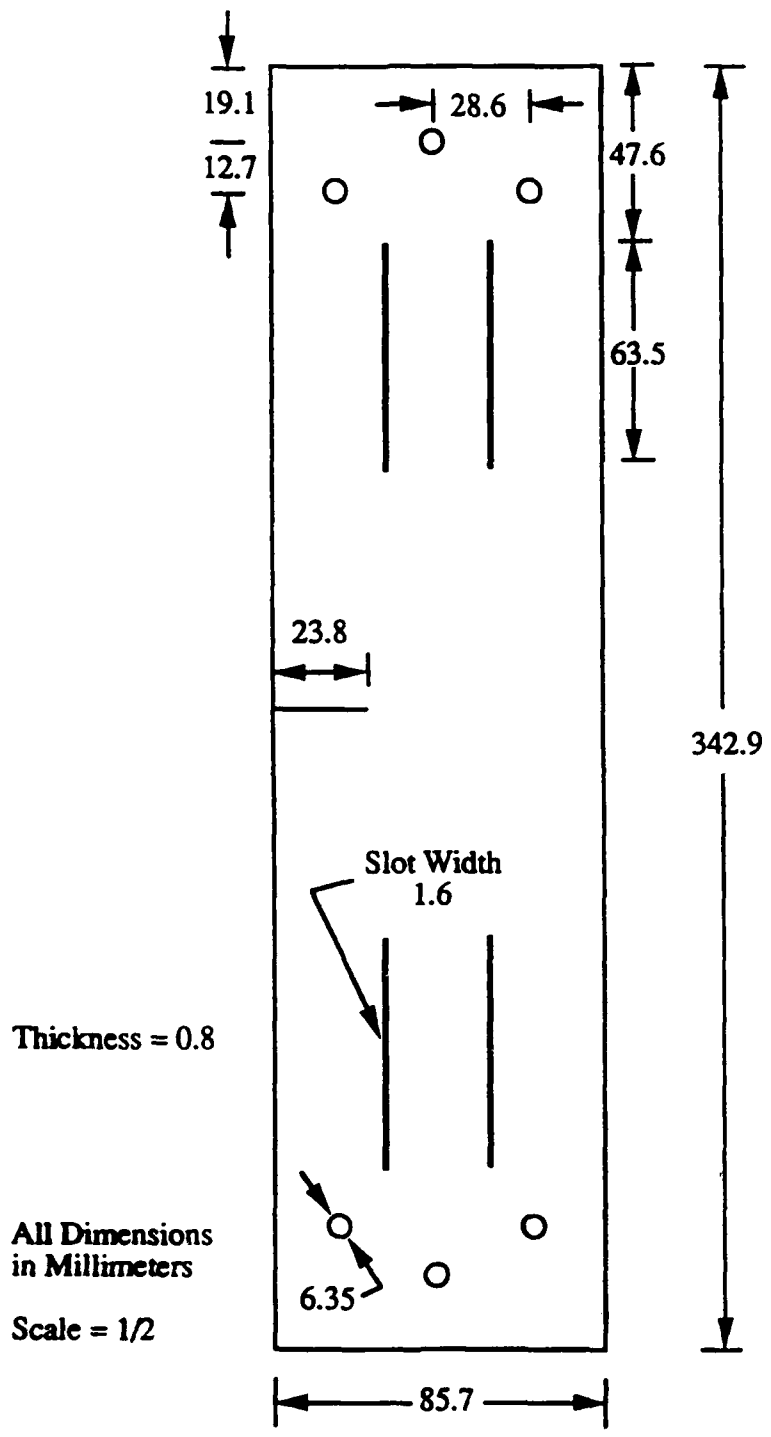


Figure 1 SEN Specimen Configuration.

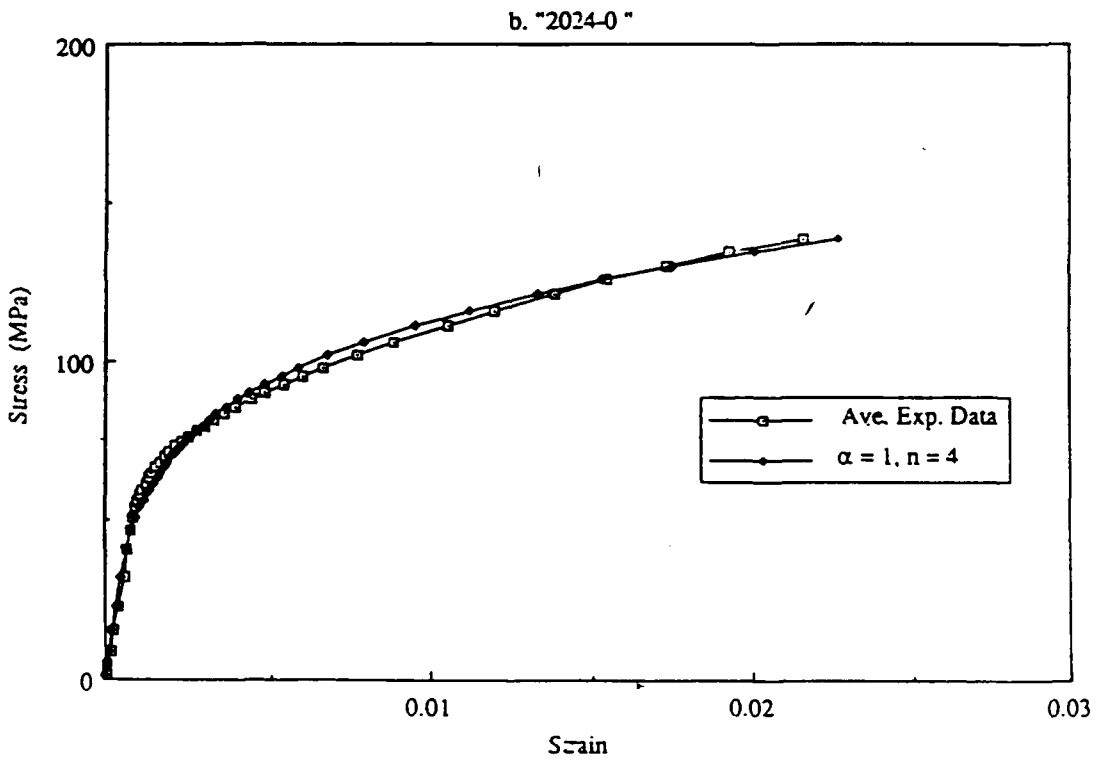
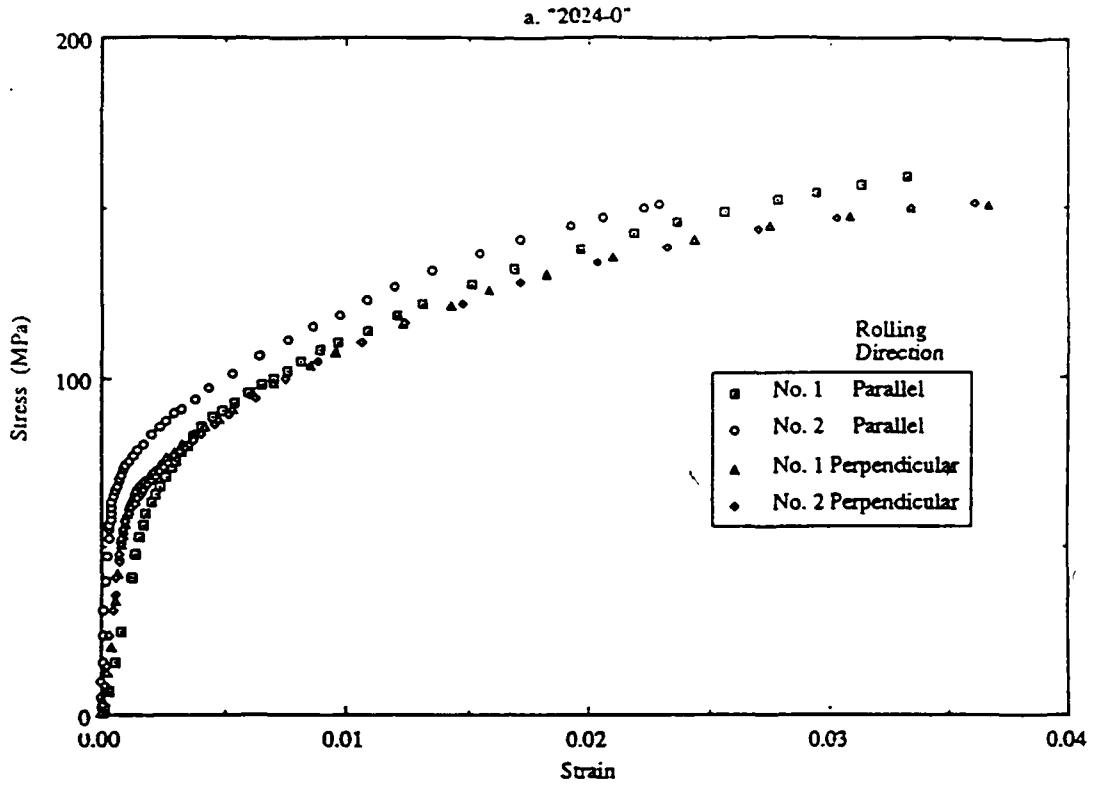


Figure 2 Uniaxial Stress-Strain Curve for 2024-0.

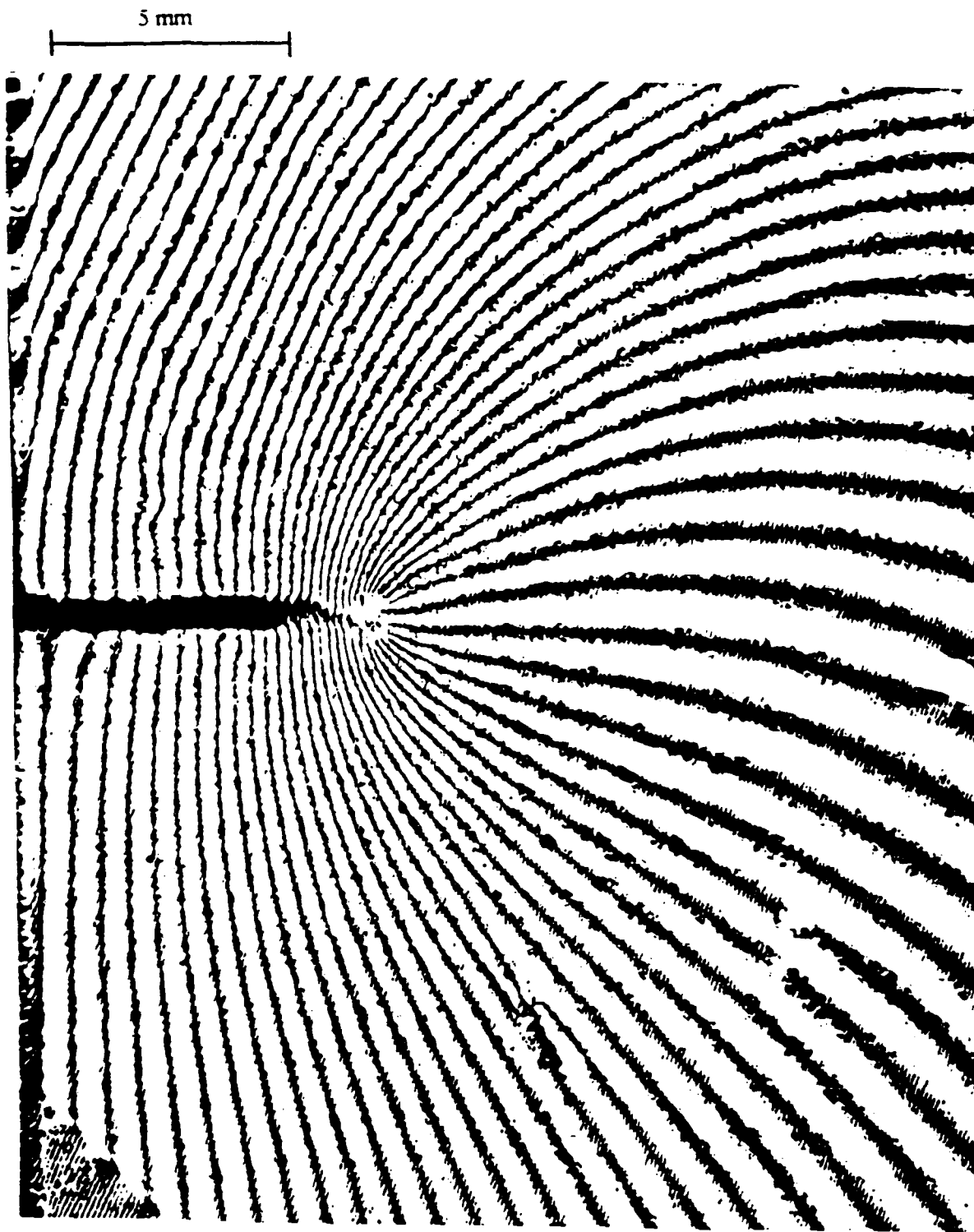


Figure 3. v-Displacement in SEN 2024-0 Aluminum Specimen. MD101988.
 $F_y = 1890$ N.

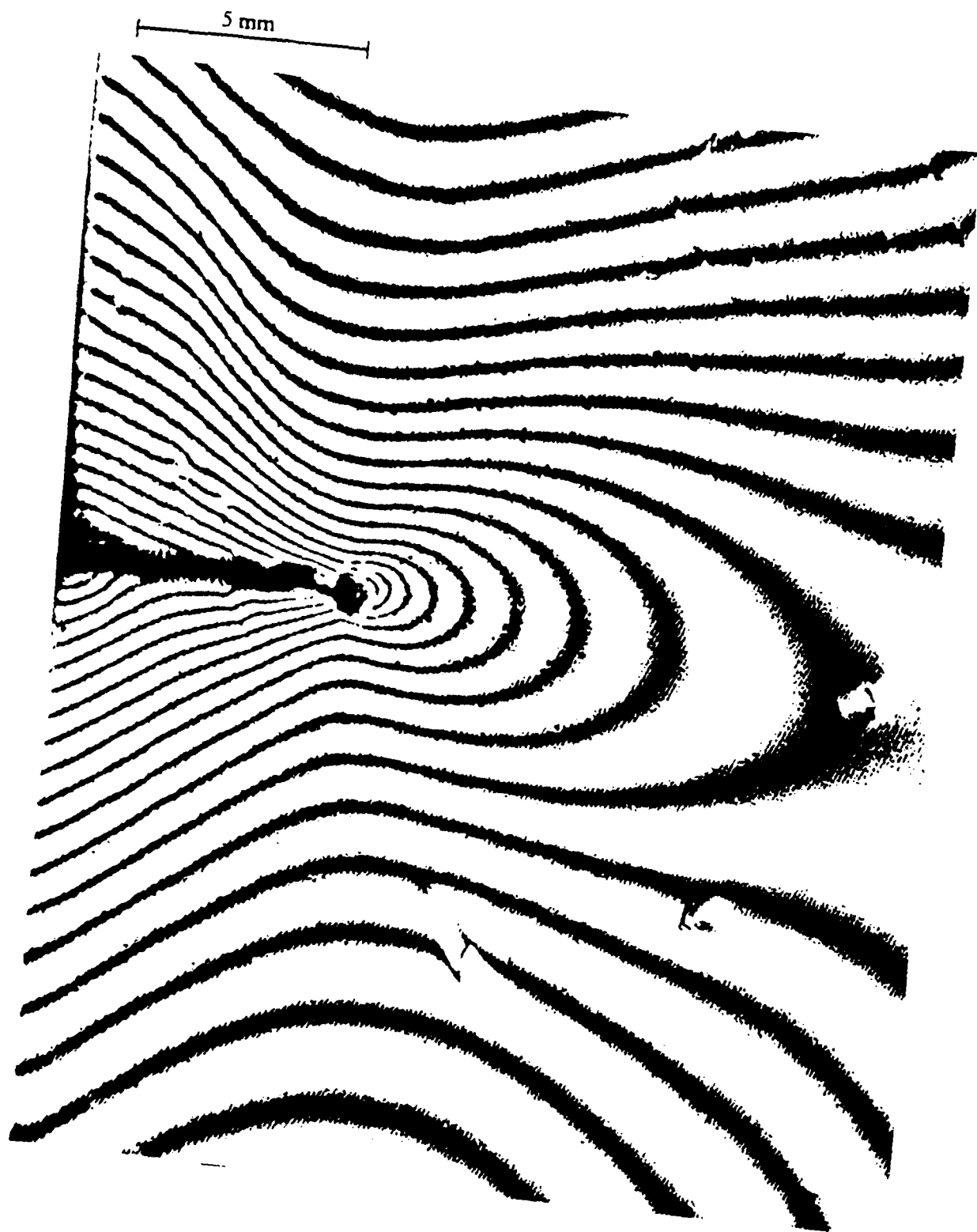


Figure 4. u-Displacement in SEN 2024-0 Aluminum Specimen. MD101988.
 $F_y = 1890 \text{ N}$.

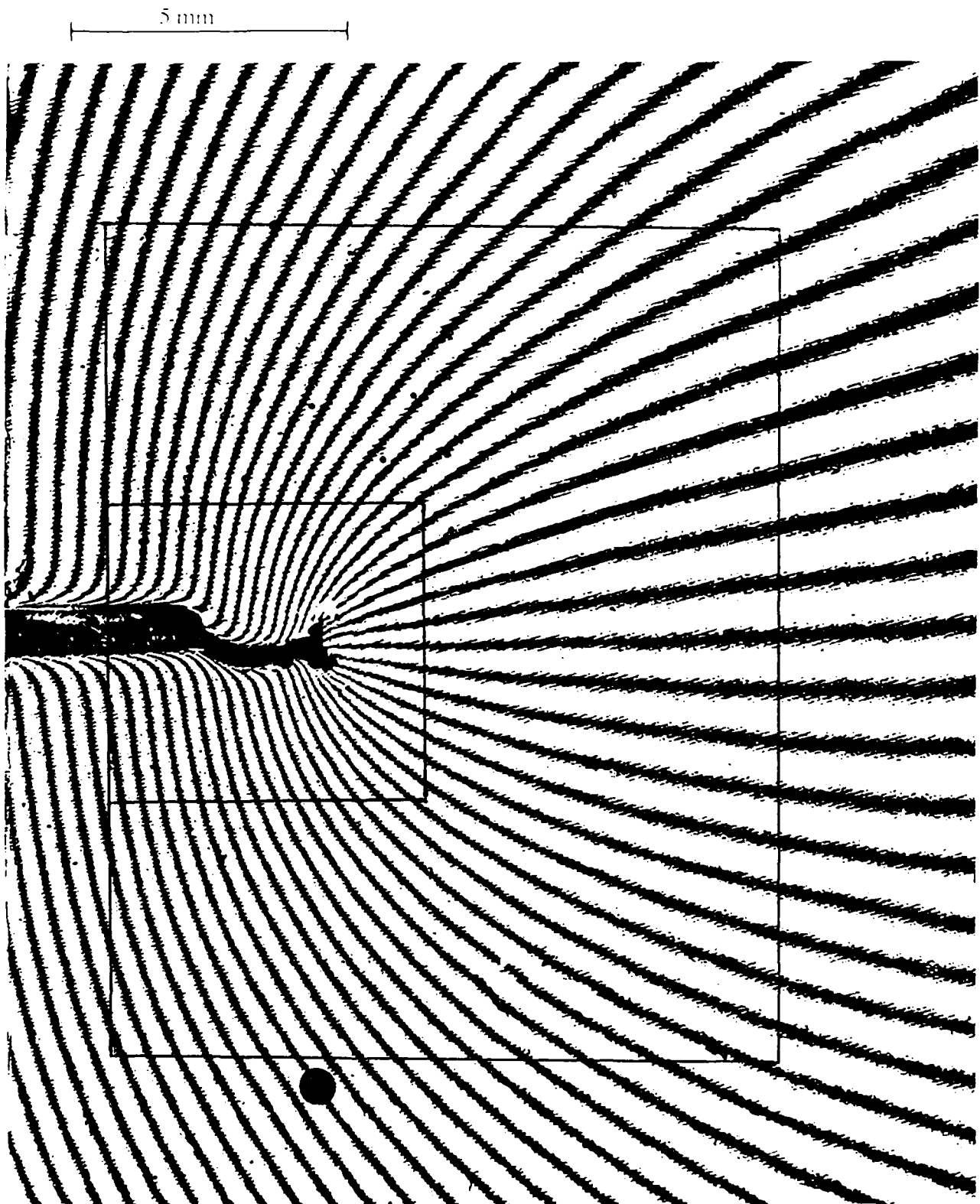


Figure 5. v -Displacement in Cruciform 2024-0 Aluminum Specimen.
MD050288. $B = 0$. $F_x = 0$, $F_y = 1695$ N.

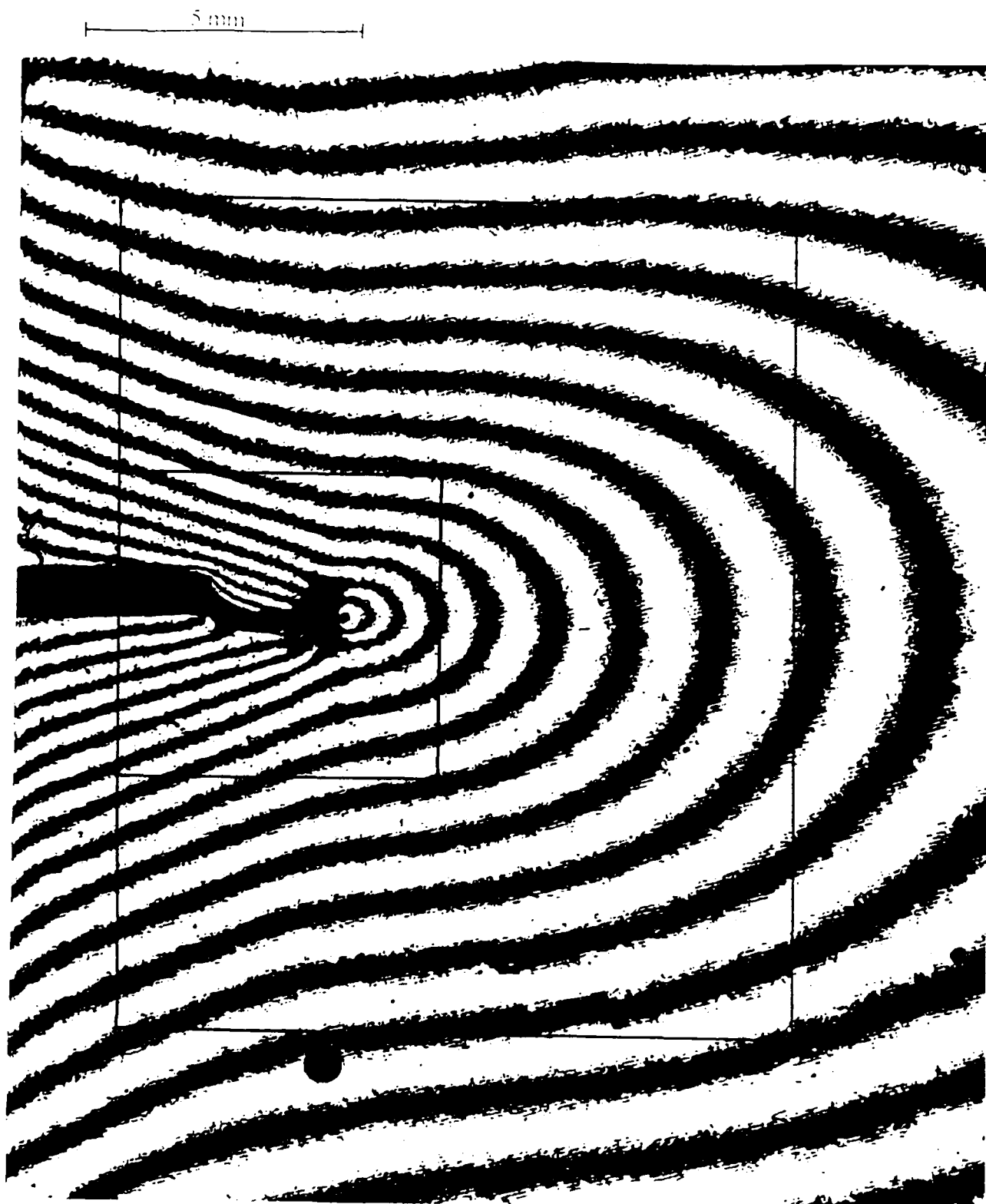


Figure 6. u -Displacement in Cruciform 2024-0 Aluminum Specimen. MD050288. $B = 0$. $F_x = 0$, $F_y = 1695$ N.

Exp. v-disp versus Δa @ $r=1.2$ mm for 2024-0

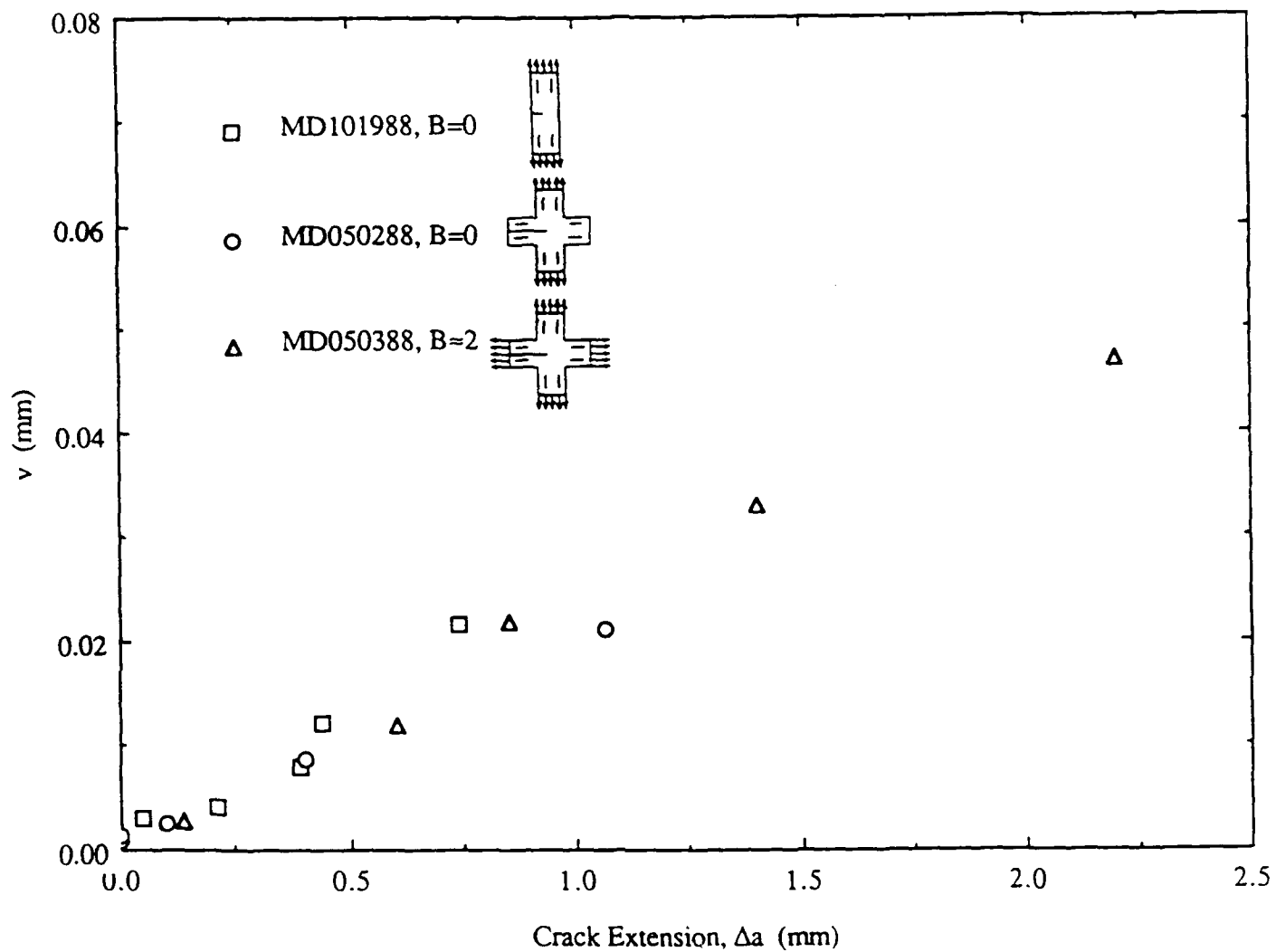


Figure 7 v-Displacement in SEN and Cruciform Specimens 2024-0 Aluminum.
 $r = 1.2$ mm, $\theta = 45^\circ$.

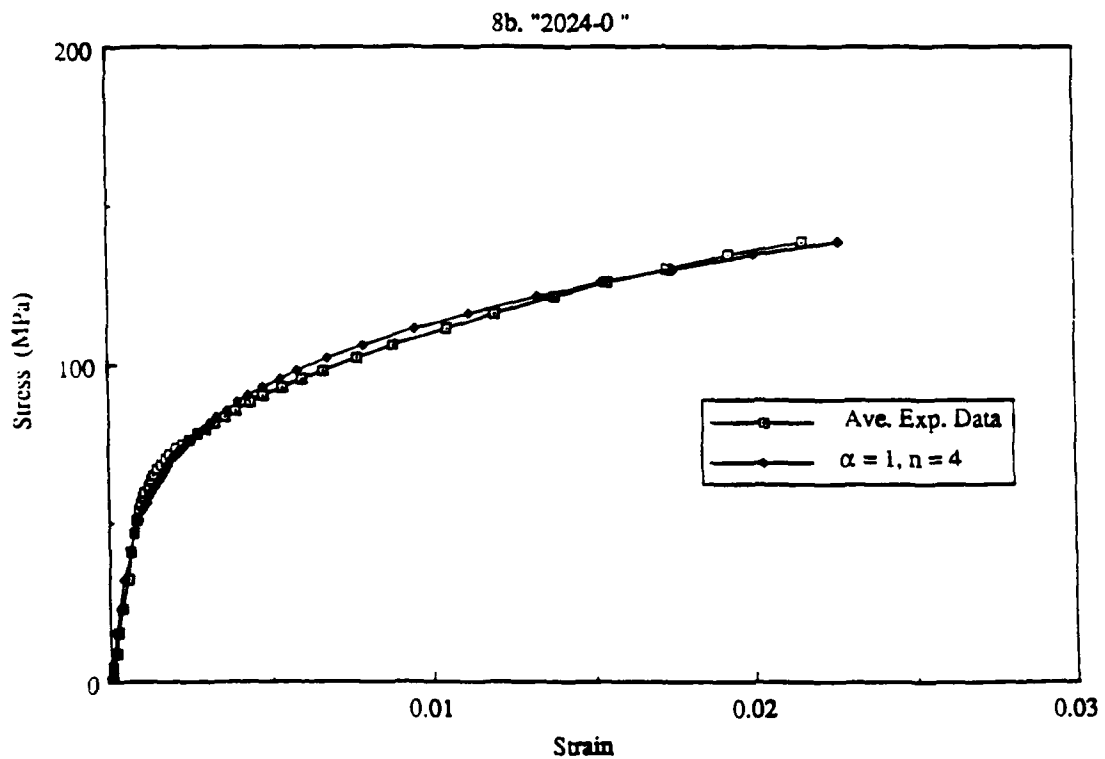
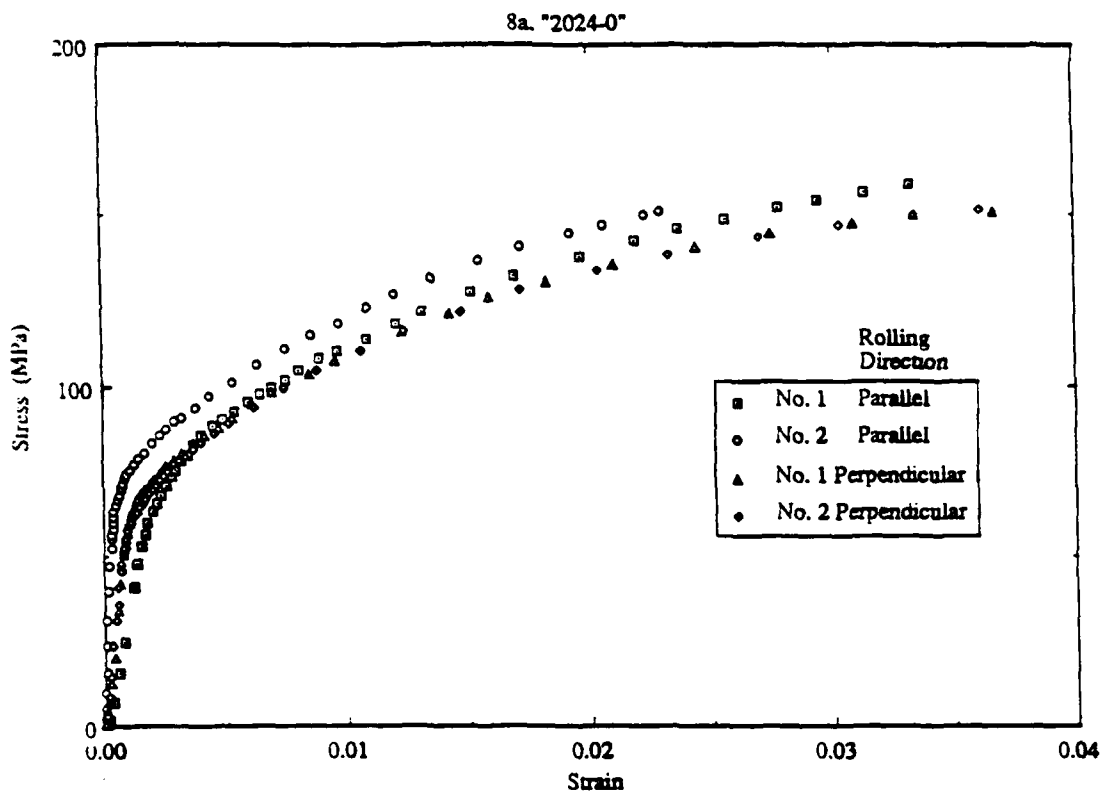


Figure 8 Uniaxial Stress-Strain Curve for 2024-0.

J vs. Load in Y Direction for 2024-0

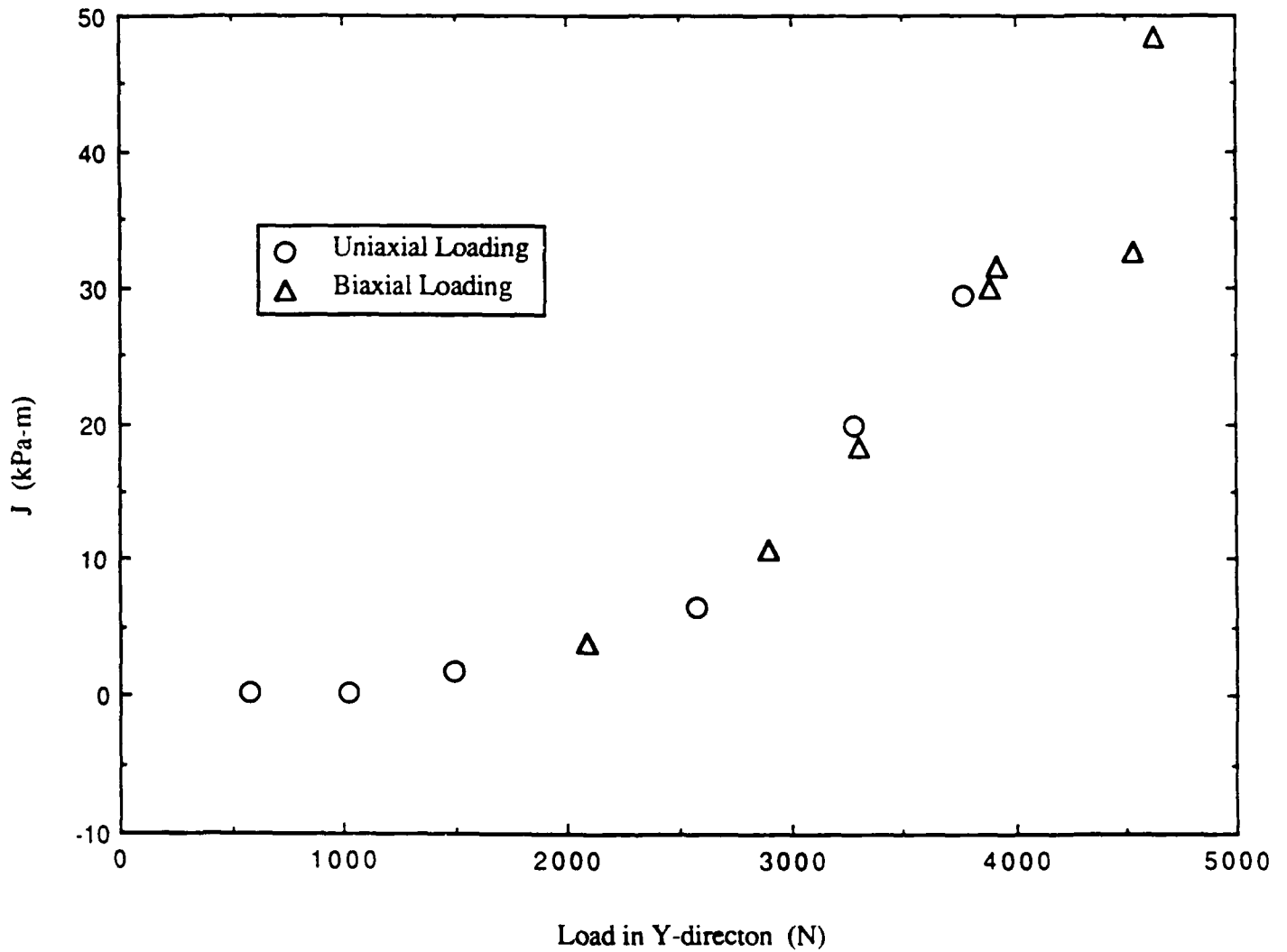


Figure 9 J Versus Applied Vertical Load, F_y , for Uniaxially and Biaxially Loaded Cruciform, 2024-0 Aluminum Specimens.

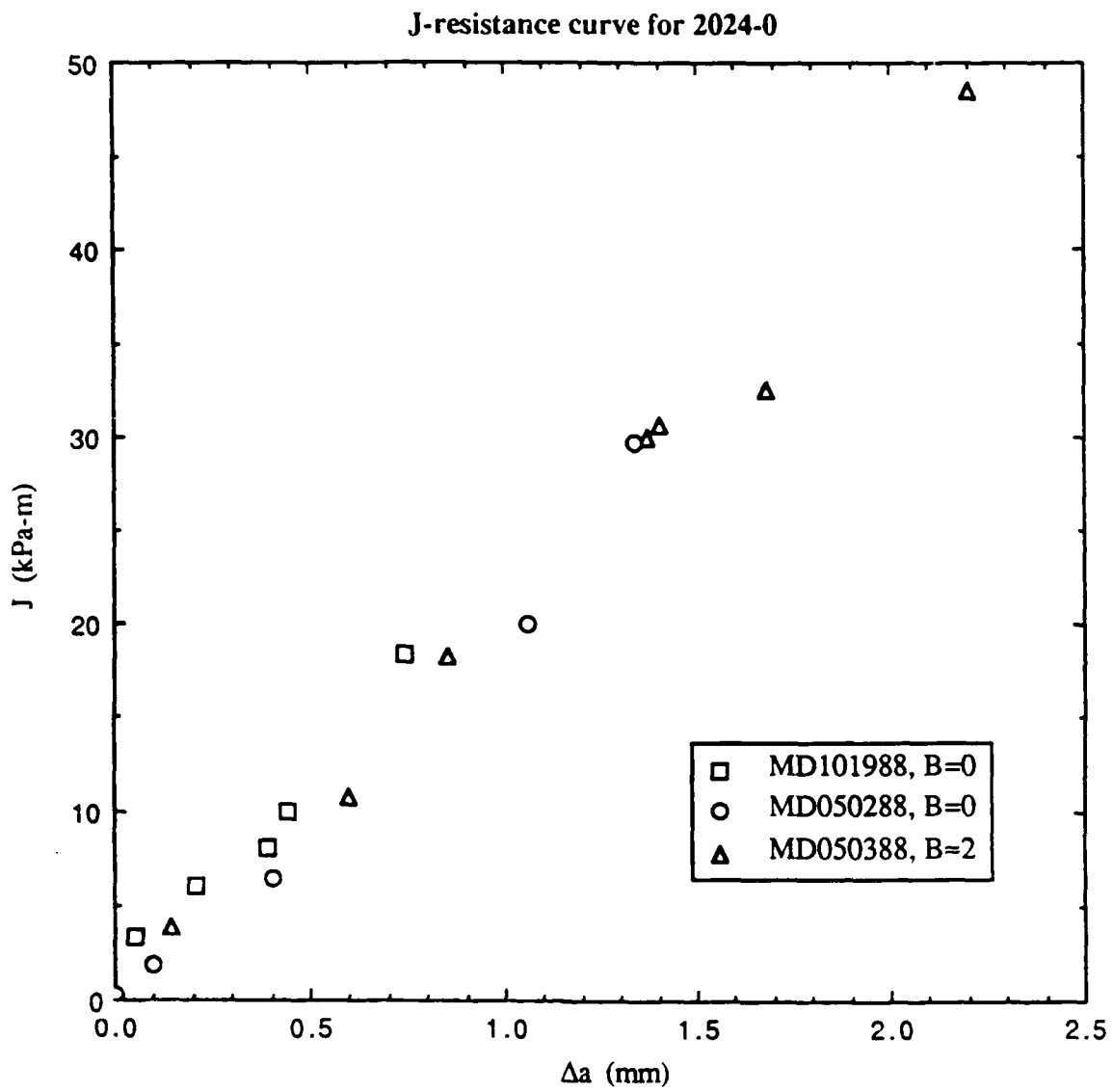


Figure 10 J-Resistance Curves for SEN and Cruciform 2024-0 Aluminum specimens.

"MD1019-2024-0, 3290 (N)"

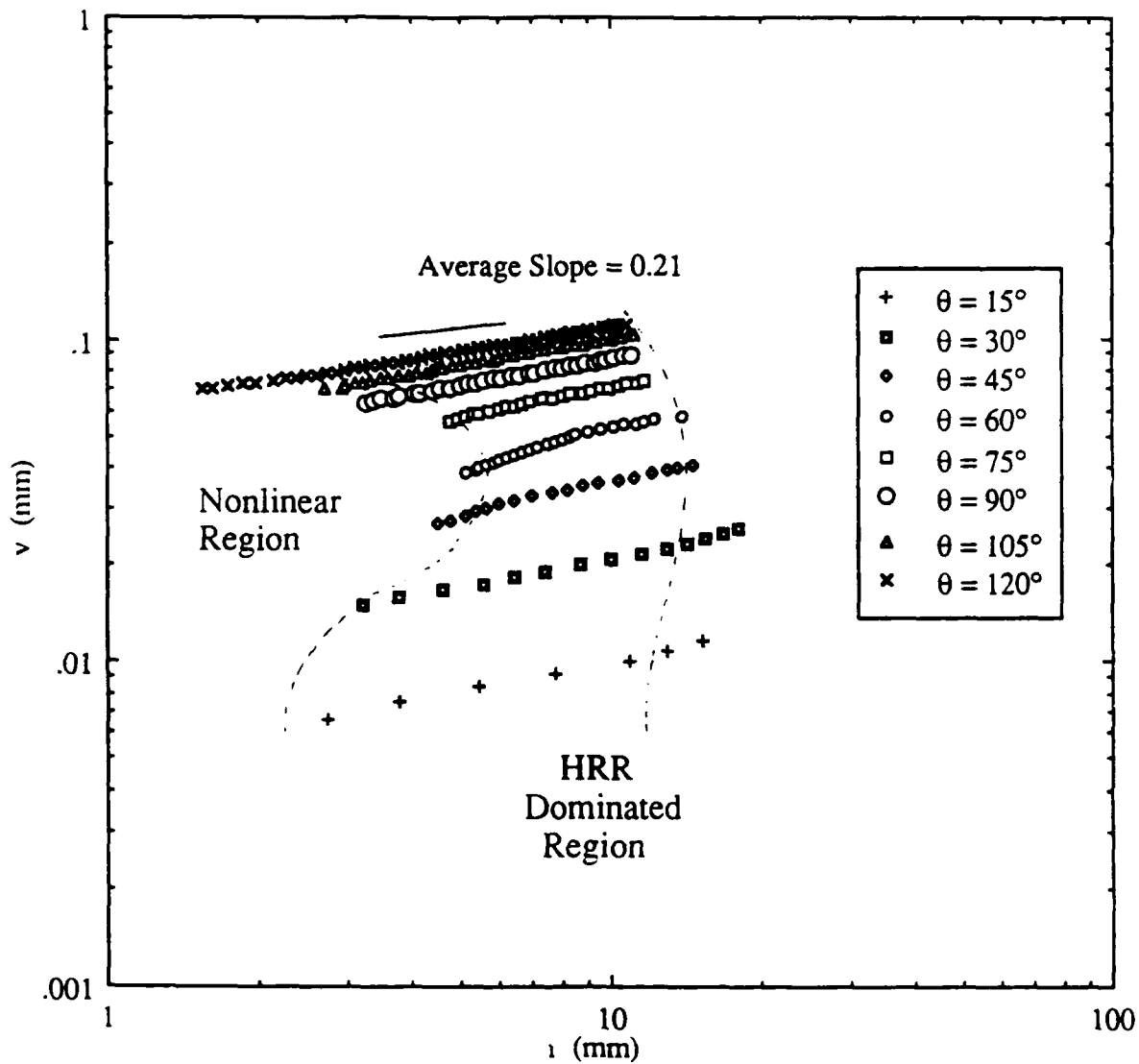


Figure 11 v -Displacement Versus r Relation for Various θ SEN 2024-0 Aluminum Specimen. $\Delta a = 0.74$ mm, $F_y = 3290$ N.

"MD101988-2024-0,3290 (N)"

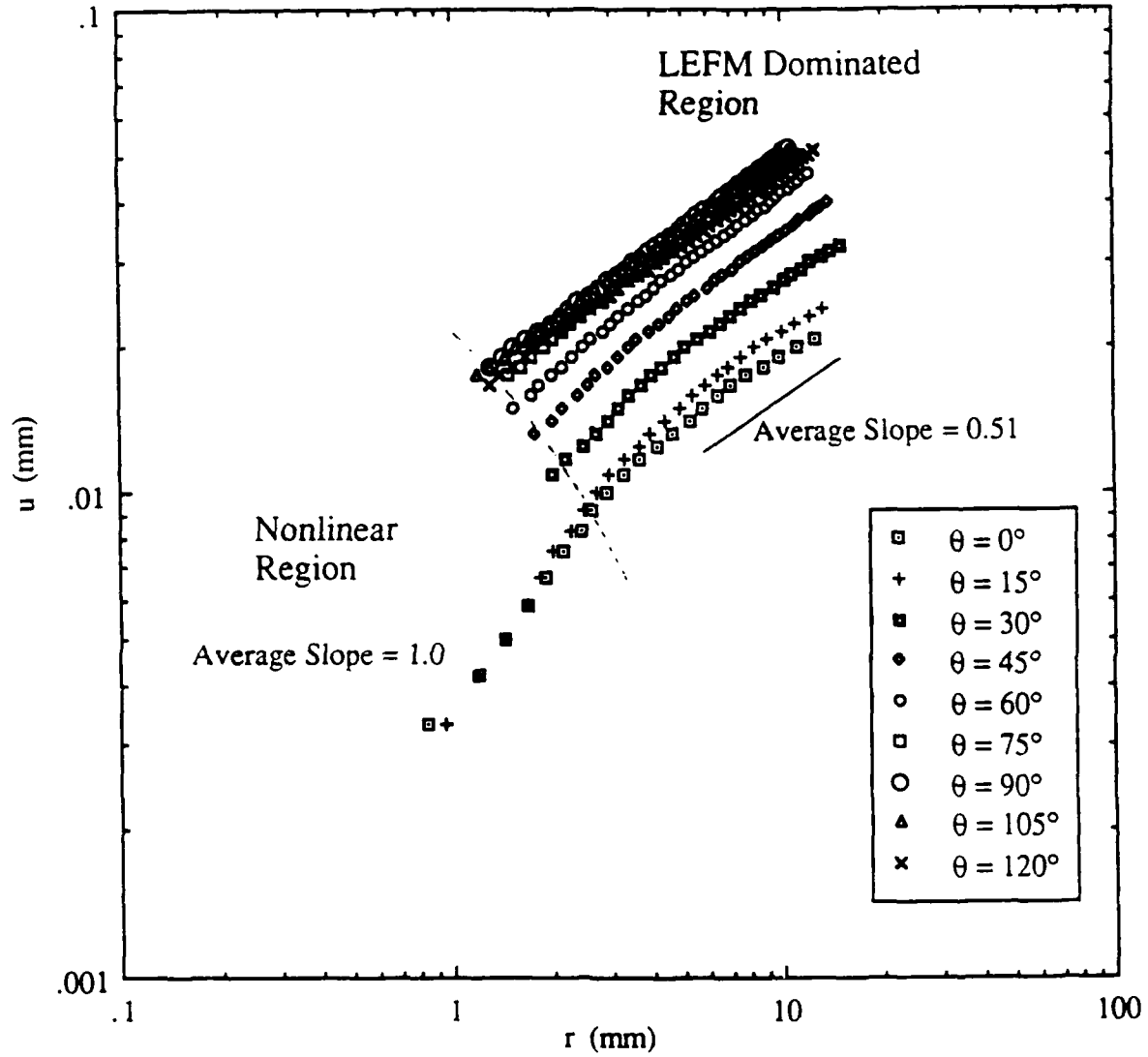


Figure 12 u-Displacement Versus r Relation for Various θ SEN 2024-0 Aluminum Specimen. $\Delta a = 0.74$ mm, $F_y = 3290$ N.

v-disp. versus Δa @ $r = 1.2$ mm for 2024-0

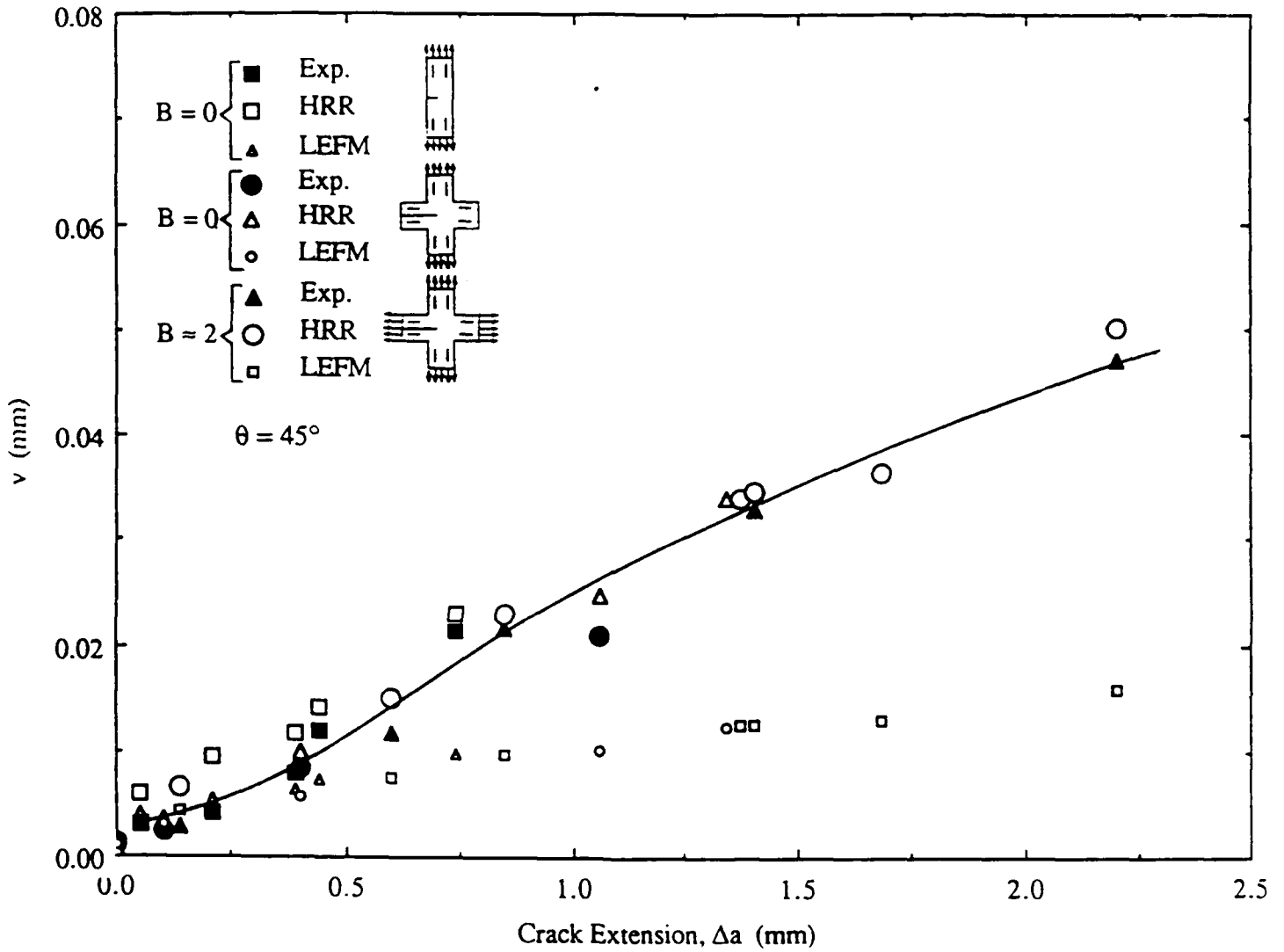


Figure 13 v-Displacements in SEN and Cruciform 2024-0 Aluminum Specimens.
 $r = 1.2$ mm, $\theta = 45^\circ$.

u-disp. versus Δa @ $r = 1.2$ mm for 2024-0

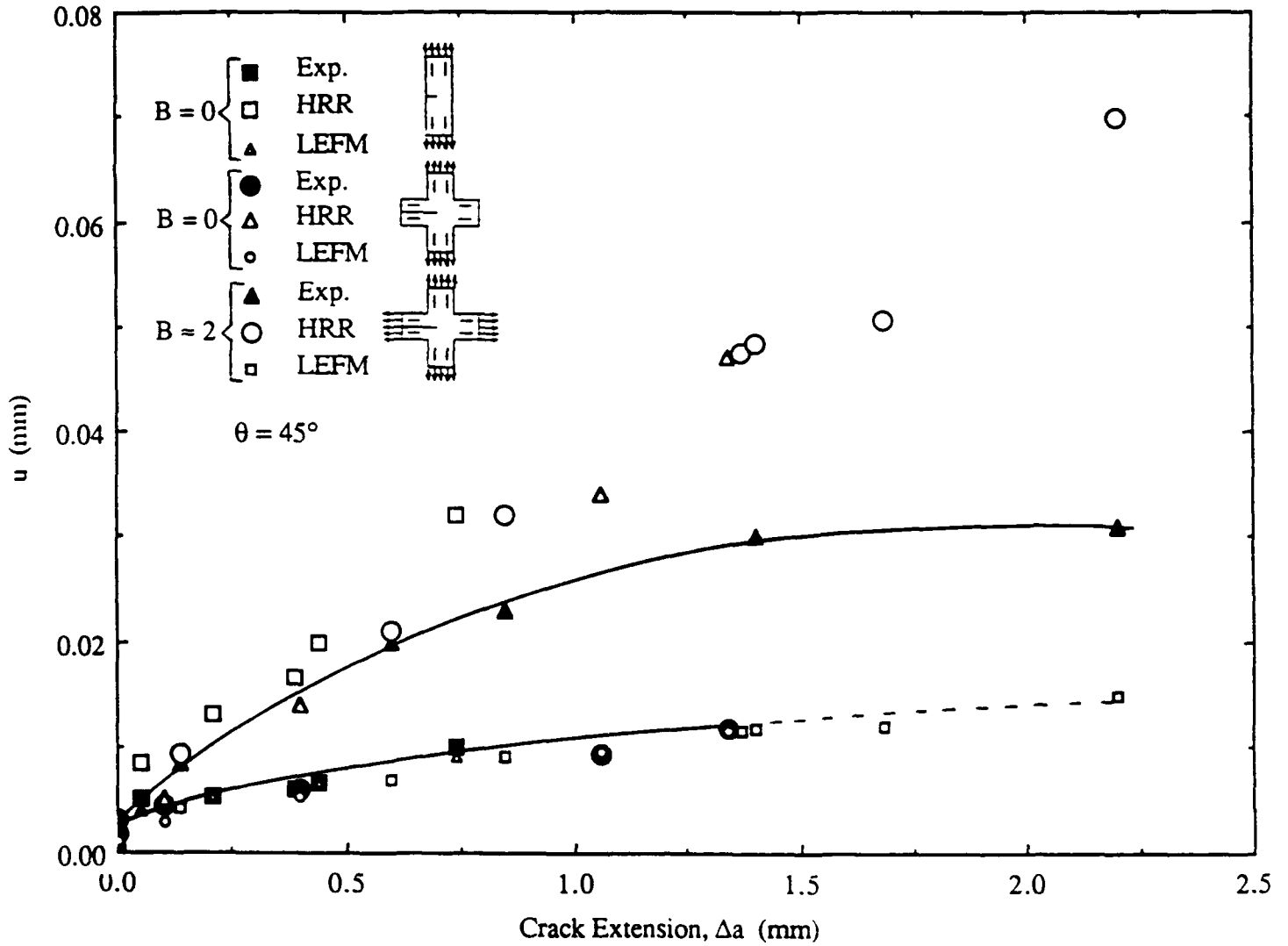


Figure 14 u-Displacements in SEN and Cruciform 2024-0 Aluminum Specimens.
 $r = 1.2$ mm, $\theta = 45^\circ$.

| | | | | |
|--|--|--|---|--|
| Office of Naval Research 800 N Quincy Street Arlington, VA 22217-5000 Attn: Code 11325M (4 copies) | Naval Surface Weapons Center White Oak, MD 20910 Attn: Code R30 Technical Library | Commander Naval Sea Systems Command Washington, DC 20362 Attn: Code 310B | Dr. M.L. Williams School of Engineering University of Pittsburgh Pittsburgh, PA 15261 | Professor J. Awerbuch Dept of Mech Engr & Mechanics Drexel University Philadelphia, PA 19104 |
| Office of Naval Research 800 N Quincy Street Arlington, VA 22217-5000 Attn: Code 1131 | Naval Surface Weapons Center Dahlgren, VA 22448 Attn: Technical Library | US Naval Academy Mechanical Engineering Dept. Annapolis, MD 21402 | Professor R.H. Gallagher President Clarkson University Potsdam, NY 13676 | Professor T.H. Lin University of California Civil Engineering Dept Los Angeles, CA 90024 |
| Defense Documentation Cntr (4 copies) Cameron Station Alexandria, VA 02314 | Naval Civil Eng Library Port Hueneme, CA 93043 Attn: Technical Library | Naval Postgraduate School Monterey, CA 93940 Attn: Technical Library | Dr. D.C. Drucker Dept. of Aerospace Eng. & Mechanics University of Florida Tallahassee, FL 32611 | Professor G.J. Dvorak Dept of Civil Engr Rensselaer Polytechnic Institute Troy, NY 12180 |
| Naval Research Laboratory Washington, DC 20375 Attn: Code 6000 | Naval Underwater Systems Center New London, CT 06320 Attn: Code 44 Technical Library | Mr. Jerome Persh Stf Specltr for Matls &Struct OUSDE & E. The Pentagon Room 301089 Washington, DC 20301 | Professor B.A. Boley Dept. of Civil Engineering Columbia University New York, NY 10025 | Dr. R.M. Christensen Chemistry & Mtrl Sci Dept Lawrence Livermore Natl Lab PO Box 80P Livermore, CA 94550 |
| Naval Research Laboratory Washington, DC 20375 Attn: Code 6300 | Naval Underwater Systems Center Newport, RI 02841 Attn: Technical Library | Professor J. Hutchinson Harvard University Div. of Applied Sciences Cambridge, MA 02138 | Professor J. Duffy Brown University Division of Engineering Providence, RI 02912 | Professor J.R. Rice Division of Applied Sciences Harvard University Cambridge, MA 02138 |
| Naval Research Laboratory Washington, DC 20375 Attn: Code 6380 | Naval Weapons Center China Lake, CA 99555 Attn: Technical Library | Dr. Harold Liebowitz, Dean School of Engr. & Applied Sci. George Washington University Washington, DC 20052 | Professor J.D. Achenbach Northwestern University Dept of Civil Engineering Evanston, IL 60208 | Professor W.N. Sharpe The Johns Hopkins University Dept of Mechanics Baltimore, MD 21218 |
| Naval Research Laboratory Washington, DC 20375 Attn: Code 5830 | NRL/Underwater Sound Reference Dept. Orlando, FL 32856 Attn: Technical Library | Professor G.T. Hahn Vanderbilt University Dept. of Mech. & Matrls. Engr. Nashville, TN 37235 | Professor F.A. McClintock Dept of Mechanical Engineering Massachusetts Institute of Technology Cambridge, MA 02139 | Professor C.F. Shih Brown University Division of Engineering Providence, RI 02912 |
| Naval Research Laboratory Washington, DC 20375 Attn: Code 6390 | Chief of Naval Operations Department of the Navy Washington, DC 20350 Attn: Code 0P-098 | Professor Albert S. Kobayashi Dept. of Mechanical Engineering University of Washington Seattle, WA 98195 | Professor D.M. Parks Dept of Mechanical Engineering Massachusetts Institute of Technology Cambridge, MA 02139 | Professor A. Rosakis California Institute of Tech Graduate Aeronautical Labs Pasadena, CA 91125 |
| David W. Taylor Naval Ship R & D Center Annapolis, MD 21402 Attn: Code 28 | Commander Naval Sea Systems Command Washington, DC 20362 Attn: Code 05R25 | Professor L.B. Freund Brown University Division of Engineering Providence, RI 02912 | Dr. M.F. Kanninen Southwest Research Institute PO Drawer 28510 6220 Culebra Road San Antonio, TX 78284 | Professor D. Post VA Polytechnic & State U Dept of Engr Science & Mechanics Blacksburg, VA 24061 |
| David W. Taylor Naval Ship R & D Center Annapolis, MD 21402 Attn: Code 2812 | Commander Naval Sea Systems Command Washington, DC 20362 Attn: Code 05R26 | Professor B. Budiansky Harvard University Division of Applied Sciences Cambridge, MA 02138 | Professor F.P. Chiang Dept of Mechanical Engr State U of NY at Stony Brook Stony Brook, NY 11794 | Professor W. Sachse Cornell University Dept of Theoretical & Applied Mechanics Ithaca, NY 14853 |
| David W. Taylor Naval Ship R & D Center Annapolis, MD 21402 Attn: Code 2814 | Commander Naval Sea Systems Command Washington, DC 20362 Attn: Code 09B31 | Professor S.N. Atluri Georgia Institute of Technology School of Engr. & Mechanics Atlanta, GA 30332 | Professor S.S. Wang Dept of Theoretical & Appl Mechs University of Illinois Urbana, IL 61801 | |
| David W. Taylor Naval Ship R & D Center Annapolis, MD 21402 Attn: Code 1700 | Commander Naval Sea Systems Command Washington, DC 20362 Attn: Code 55Y | Professor G.Springer Stanford University Dept. of Aeronautics & Astronautics Stanford, CA 94305 | Professor Y. Weitsman Civil Engr Department Texas A&M University College Station, TX 77843 | |
| David W. Taylor Naval Ship R & D Center Annapolis, MD 21402 Attn: Code 1720 | Commander Naval Sea Systems Command Washington, DC 20362 Attn: Code 55Y2 | Professor H.T. Hahn Dept of Engr Sciences & Mech Penn State University 227 Hammond Bldg University Park, PA 16802 | Professor I.M. Daniel Dept of Mechanical Engr Northwestern University Evanston, IL 60208 | |
| David W. Taylor Naval Ship R & D Center Annapolis, MD 21402 Attn: Code 1720.4 | Commander Naval Sea Systems Command Washington, DC 20362 Attn: Code 03D | Professor S.K. Datta University of Colorado Dept. of Mechanical Engineering Boulder, CO 80309 | Professor C.T. Sun School of Aeronautics & Astronautics Purdue University W. Lafayette, IN 47907 | |
| Naval Air Development Center Warminster, PA 18974 Attn: Code 6043 | Commander Naval Sea Systems Command Washington, DC 20362 Attn: Code 7226 | | | |
| Naval Air Development Center Warminster, PA 18974 Attn: Code 6063 | Commander Naval Sea Systems Command Washington, DC 20362 Attn: Code 310A | | | |

| REPORT DOCUMENTATION PAGE | | READ INSTRUCTIONS BEFORE COMPLETING FORM |
|--|-----------------------|--|
| 1. REPORT NUMBER 89-J-1276 | 2. GOVT ACCESSION NO. | 3. RECIPIENT'S CATALOG NUMBER |
| 4. TITLE (and Subtitle) HRR Field in an Aluminum SEN Specimen | | 5. TYPE OF REPORT & PERIOD COVERED |
| | | 6. PERFORMING ORG. REPORT NUMBER UWA/DME/TR-89/63 |
| 7. AUTHOR(s) M.S. Dadkhah and A.S. Kobayashi | | 8. CONTRACT OR GRANT NUMBER(s) N00014-89-J-1267 |
| 9. PERFORMING ORGANIZATION NAME AND ADDRESS Department of Mechanical Engineering, FU-10 University of Washington Seattle, Washington 98195 | | 10. PROGRAM ELEMENT, PROJECT, TASK AREA & WORK UNIT NUMBERS |
| 11. CONTROLLING OFFICE NAME AND ADDRESS Office of Naval Research Arlington, Virginia 22217 | | 12. REPORT DATE April 1989 |
| | | 13. NUMBER OF PAGES 18 |
| 14. MONITORING AGENCY NAME & ADDRESS (if different from Controlling Office) | | 15. SECURITY CLASS. (of this report) Unclassified |
| | | 15a. DECLASSIFICATION/DOWNGRADING SCHEDULE |
| 16. DISTRIBUTION STATEMENT (of this Report) Unlimited | | |
| 17. DISTRIBUTION STATEMENT (of the abstract entered in Block 20, if different from Report) | | |
| 18. SUPPLEMENTARY NOTES | | |
| 19. KEY WORDS (Continue on reverse side if necessary and identify by block number) Moire Interferometry, Elastic-plastic Fracture Mechanics, J-Resistance Curve | | |
| 20. ABSTRACT (Continue on reverse side if necessary and identify by block number) Moire interferometry was used to record simultaneously the vertical and horizontal displacements associated with stable crack growth in single edge notched, 2024-O Aluminum specimens. For a small stable crack growth of 1.5 mm, the vertical displacement showed the dominance of the HRR field but the horizontal displacement deviated from the HRR field at the early stage of loading. | | |

END

6-89

DTIC